Title: Insights into cell wall structure of *Sida hermaphrodita* and its influence on recalcitrance

Journal: Carbohydrate Polymers

Authors:

Tatjana Damm [1,2x]

Sivakumar Pattathil [3x]

Markus Günl [4]

Nicolai David Jablonowski [2,4]

Malcolm O'Neill [3]

Katharina Susanne Grün [1]

Philipp Michael Grande [5]

Walter Leitner [5,6]

Ulrich Schurr [2,4]

Björn Usadel [1,2,4]

Holger Klose [1,2*]

Abstract:

The perennial plant *Sida hermaphrodita* (Sida) is attracting attention as potential energy crop. Here, the first detailed view on non-cellulosic Sida cell wall polysaccharide composition, structure and architecture is given. Cell walls were prepared from Sida stems and sequentially extracted with aqueous buffers and alkali. The structures of the quantitatively predominant polysaccharides present in each fraction were determined by biochemical characterization, glycome profiling and mass spectrometry. The amounts of glucose released by Accellerase-1500® treatment of the cell wall and the cell wall residue remaining after each extraction were used to assess the roles of pectin and hemicellulose in the recalcitrance of Sida biomass.

4-*O*-methyl glucuronoxylan with a low proportion of side substitutions was identified as the major non-cellulosic glycan component of Sida stem cell walls. Pectic polysaccharides and xylans were found to be associated with lignin, suggesting that these polysaccharides have roles in Sida cell wall recalcitrance to enzymatic hydrolysis.

Keywords:

Sida hermaphrodita, plant cell wall, non-cellulosic polysaccharides, glucuronoxylan, pectin, lignocellulose utilization.

Abbreviations:

AG	arabinogalactan
AIR	alcohol-insoluble residue
Ara	arabinose
Ara(*f*)	arabinose (furanose)
CrC	crystalline cellulose
ELISA	enzyme-linked immunosorbent assay
Fuc	fucose
Gal	galactose
GalA	galacturonic acid
Glc	glucose
GlcA	glucuronic acid
HG	homogalacturonan
HM	heteromannan
HPAEC-PAD	high-performance anion exchange chromatography with pulsed amperometric detection
MALDI-TOF-MS	matrix-assisted laser-desorption time-of-flight mass spectrometry
Man	mannose
MPS	matrix polysaccharide
RG	rhamnogalacturonan
Rha	rhamnose
t-	terminal
TFA	trifluoroacetic acid
X	xylan
XEG	xyloglucan-specific endo-β-1,4-glucanase
XG	xyloglucan
Xyl	xylose
XXFG/XLFG/XLFG/ XXXG/XXLG/XLXG	xyloglucan oligosaccharides

1 Introduction

Lignocellulosic biomass is comprised predominantly of plant cell walls, and is an abundant and sustainable resource for the production of chemicals and biofuels. Many studies have assessed the potential of crop plants, including maize, for energy production (Fornalé et al., 2012; Tollenaar & Lee, 2002). To minimize competition with food production, there is increasing interest in using perennial, non-food plants including *Silphium perfoliatum*, Szarvasi and Miscanthus (Mast et al., 2014; De Souza 2015). This is especially true for crops with potential to serve as high yielding lignocellulose producer, such as *Sida hermaphrodita* (L.) Rusby (hereafter referred to as Sida), also known by the common names Virginia fanpetals and Virginia mallow (Borkowska & Molas, 2013; Borkowska, Molas, & Kupczyk, 2009; Kocoń & Matyka, 2012; Šiaudinis et al., 2015). Sida has been investigated systematically since the 1950s, mainly in Poland, where the plant was first introduced to Europe. These studies focused on plant cultivation for biomass production (Borkowska & Molas, 2012, 2013; Borkowska et al., 2009; Slepetys, Kadziuliene, Sarunaite, Tilvikiene, & Kryzeviciene, 2012) and achieved biomass yields of up to 13.0 tonnes of Sida dry matter per hectare (Borkowska & Molas, 2012).

To date, little is known about Sida cell wall composition and structure. General parameters have been described for Sida biomass including crude ash, protein, fibre, fat, acid detergent lignin, etc. (Franzaring, Holz, Kauf, & Fangmeier, 2015), acetyl bromide-soluble lignin, crystalline cellulose and matrix polysaccharide (MPS) content (Jablonowski et al., 2016). Generally, the function of lignin and the MPS network is shown to crosslink/anchor the cellulose microfibril scaffold and is known to contribute to cell wall stability and lignocellulose recalcitrance (Scheller & Ulvskov, 2010).

Sustainable processing of lignocellulose, meaning the usage of carbohydrates and lignin as renewable intermediates for value-added products, requires overcoming recalcitrance to enable economically viable processes and thereby lower investment costs (Himmel et al., 2007; Himmel & Picataggio, 2008; Silveira, Stoyanov, Gusarov, Skaf, & Kovalenko, 2013).

The structure and composition of plant cell walls are important factors that determine lignocellulose recalcitrance (Damm, Commandeur, Fischer, Usadel, & Klose, 2016). These factors have a high impact on the saccharification and fermentation of lignocellulosic biomass. Within the cell wall, MPS have been shown to have an important role/s in contributing to biomass recalcitrance (DeMartini et al., 2013a). A reduction of xylan *O*-acetylation has been suggested to enhance lignocellulose recalcitrance in Arabidopsis (Xiong, Cheng, & Pauly, 2013). In contrast, arabinose substitutions of xylan are shown to enhance saccharification by negatively affecting cellulose crystallinity in Miscanthus (F. Li et al., 2013). Structural features including the pattern of branching or substitution of matrix glycans have also been reported to have an impact on subsequent processing of lignocellulosic biomass (De Souza et al., 2015; Silveira et al., 2013).

In this study, we have determined the predominant types of non-cellulosic polysaccharides present in the stem cell walls of field-grown Sida. Additionally we show enzymatic hydrolysis data for Sida and discuss which cell wall components impact recalcitrance in Sida.

2 Materials and methods

2.1 Plant material

Sida seeds were provided by Marcel Hohmeyer (Sida World) and Marek Bury (West Pomeranian University of Technology, Department of Agronomy, Szeczecin, Poland). Sida plants were pre-cultivated in a greenhouse and grown in a field in Mersch, Germany [100 m o. NN, 6°22’34 East and 50°57’50 North using the european terrestrial reference system 1989 (Jablonowski et al., 2016)]. Above ground five two-years-old shoots were randomly harvested at the same time point in Sep. 2015 from different plants displaying different thickness.

2.2 Preparation of alcohol insoluble residue and sequential extraction of cell wall polysaccharides

Sida shoot sections of 10 cm in length were used to prepare the alcohol-insoluble residue (AIR). AIR was prepared according to Pattathil *et al*. (Pattathil, Avci, Miller, & Hahn, 2012) with a small modification regarding the grinding. Plant material was ground in ice-cold aq. 80% (v/v) ethanol (100 ml per g plant material) using a pre-cooled blender (Waring Blender HGB25E). For glycome profiling studies dried AIR was extracted according to (Pattathil et al., 2012). For all other analyses the AIR was ground to a fine powder in a 50 ml metal jar containing one 24 mm stainless steel ball bearing using a ball mill (Retsch MM 400) for 2 min at a frequency setting of 30 s^{-1}.

Sequential cell wall polysaccharide extraction was carried out according to Pattathil *et al.* (Pattathil et al., 2012) using 50 mM ammonium oxalate $(NH_4)_2C_2O_4$, 50 mM sodium carbonate Na_2CO_3 containing 0.5% (w/v) sodium borohydride $NaBH_4$, 1 M potassium hydroxide (KOH) containing 1% (w/v) sodium borohydride, 4 M KOH, 207 mM sodium chlorite ($NaClO_2$) with 0,75% (w/v) with glacial acetic acid (at 70^{o}C) and finally with 4 M KOH (post chlorite) containing 1% (w/v) sodium borohydride. 2-propanol or 2-octanol was added to the alkali extracts prior to neutralization to reduce foaming. All neutralized extracts were subjected to dialysis and were dried by AIR flow or lyophilization. The amounts of material recovered at each extraction steps were determined gravimetrically.

2.3 Monosaccharide composition analysis

The monosaccharide composition of each cell wall extract was determined. 200-300 µl of dialyzed extracts were mixed (1:1 (v/v)) with 4 M trifluoroacetic acid (TFA) and hydrolyzed for 90 min at 121°C (Foster, Martin, & Pauly, 2010b). Samples were dried using a flow of air and the residue was then dissolved in ultrapure water for analysis.

Monosaccharide analysis was performed according to Voiniciuc et al. (Voiniciuc et al., 2015) using high-performance anion exchange chromatography with pulsed amperometric

detection (HPAEC-PAD). A CarboPac^{TM} PA20 column (3 x 150 mm, Thermo Scientific) was used for the separation of monosaccharides. The column was equilibrated with 2 mM NaOH for 10 min before sample injection. Neutral sugars were separated with 2 mM NaOH over 25 min. This was followed by 550 mM NaOH for 10 min to separate uronic acids and then by 800 mM NaOH for 10 min to regenerate the column. All steps were performed at a flow rate of 0.5 ml min^{-1}. Monosaccharide amounts were normalized to the internal standard (2-deoxy-D-glucose) and quantified using standard concentration curves.

2.4 Cellulose content determination

The crystalline cellulose content of the AIR was determined after hydrolyzing and removing the non-crystalline cellulose with acetic and nitric acid (Updegraff, 1969). The remaining crystalline cellulose residue was hydrolyzed with 72% (w/v) sulfuric acid. Carbohydrate content was determined using the Anthrone assay (Scott & Melvin, 1953).

2.5 Lignin determination

Acetyl bromide soluble lignin (ABSL) was measured directly from AIR according to Foster et al. (Foster, Martin, & Pauly, 2010a) using the acetyl bromide spectrophotometric method. Instead of a predefined coefficient, for each measurement different amounts (0.1 to 0.7 mg) of Kraft-Lignin (Sigma-Aldrich, Seelze, Germany) were included as an external standard.

2.6 Glycosyl-linkage composition analysis of sequentially extracted cell wall polysaccharides

Glycosyl-linkage analysis was carried out essentially as previously described (Voiniciuc et al., 2015). 1-10 mg dried polysaccharides were dissolved in 2.2 ml water and a portion (200 µl) was used for monosaccharide analysis. The remaining material was acidified by adding 600 µl 0.1 M sodium acetate, pH 4.6. Uronic acids were then carboxyl-reduced to their corresponding 6,6-dideuterio derivatives as described (Gibeaut & Carpita, 1991; Huang et al., 2011). For reduction, 0.1 mg 1-cyclohexyl-3-(2-morpholinyl-4-ethyl) carbodiimide (methyl-p-toluene sulfonate) was added to the samples. After 2h at room temperature, 0.1

mg sodium borodeuteride together with 1 ml cold 2 M imidazole, pH 7.0, was added and the sample was kept on ice for another hour. Glacial acetic acid was then added drop-wise to destroy the residual sodium borodeuteride. The carboxyl-reduced samples were extensively dialyzed against water and then lyophilized. The dry samples were solubilized in 200 µl anhydrous DMSO and methylated using NaOH as described by Gille *et al.* (Gille, Hänsel, Ziemann, & Pauly, 2009). A suspension of NaOH in DMSO was prepared using 100 µl 50% (w/w) sodium hydroxide that was washed and sonicated several times with anhydrous DMSO (5 ml) and finally suspended in 2 ml anhydrous DMSO. The NaOH-DMSO suspension (200 µl) together with methyl iodide (100 µl) was added to samples. After 3 h at room temperature, 2 ml water was added to quench the reaction and methylated polysaccharides were then extracted with 2 ml dichloromethane. Methylated polysaccharides were hydrolyzed (250 µl of 2 M TFA), the released monosaccharides reduced to their alditols with sodium borodeuteride and then converted to their corresponding alditol acetate derivatives and analyzed by GC-MS as previously described (Foster et al., 2010b).

2.7 Glycome profiling of sequentially extracted cell wall polysaccharides

Glycome profiling of the ammonium oxalate, sodium carbonate, 1M KOH, 4M KOH, chlorite and 4M KOHPC (KOH post chlorite) extracts was performed using a comprehensive suite of plant cell wall glycan-directed monoclonal antibodies (mAbs) using the methods described in Pattathil *et al* (Pattathil et al., 2012). The extracts were diluted to 20 µg ml^{-1} carbohydrate and portions (15 µl $well^{-1}$) were coated onto 384 well plastic plates (Costar 3700, Corning Inc., Corning, NY, USA). ELISA was then performed using a Robotic system (Thermo Fisher Scientific Inc. Waltham, MA, USA). The enzyme-linked immunosorbent assay (ELISA) responses of each mAbs are represented as heat maps. Glycan-directed mAbs used in glycome profiling analyses were obtained from laboratory stocks (CCRC, JIM and MAC series) at the Complex Carbohydrate Research Center (available through CarboSource Services; http://www.carbosource.net) or from BioSupplies (Australia) (BG1, LAMP).

2.8 MALDI-TOF mass spectrometric analyses of xyloglucan and glucuronoxylan oligosaccharides

Xyloglucan oligosaccharides were generated by treating solutions of the 4M KOH-soluble materials in 50 mM ammonium formate, pH 5, with a xyloglucan-specific endo-β-1,4-glucanase (XEG) as previously described (Pauly et al., 1999). Glucuronoxylan oligosaccharides were generated by treating solutions of the 4M KOH-soluble materials in 50 mM ammonium formate, pH 5, with an endoxylanase (1 unit, M1, Megazyme, County Wicklow, Ireland). Ethanol was added to the enzymatic digests to 70% (v/v) and the mixture kept for 24 h at 4°C. The precipitate that formed was removed by centrifugation and the soluble fraction concentrated to dryness. The residue was dissolved in water (500 µl) and then freeze-dried to remove residual ammonium formate. The residue was then dissolved in water (1 ml) and the oligosaccharides enriched using graphitized carbon (Packer, Lawson, Jardine, & Redmond, 1998). SupelcleanTM ENVITM-Carb cartridges (1 ml) were conditioned by washing with aq. 80% (v/v) acetonitrile containing 0.1% (v/v) trifluroacetic acid (TFA, 2 ml) and then with deionized water (5 ml). Solutions (1 ml) of the oligosaccharides were applied and the bound material washed with water (2 ml). The oligosaccharides were then eluted with aq. 50% acetonitrile containing 0.1% TFA (3 ml). The solutions were concentrated to dryness under a flow of warm air, the residue was dissolved in water (100 - 300 µl) and analyzed by matrix-assisted laser-desorption time-of-flight mass spectrometry (MALDI-TOF-MS).

MALDI-TOF-MS was performed in the positive-ion mode using a Bruker Microflex LT mass spectrometer and workstation (Bruker, Billerica, MA USA). Solutions (5 µl) of the oligosaccharides (~1 mg ml^{-1} in water) were mixed with an equal volume of 10 mM NaCl. A portion of this mixture (1 µl) was then added to matrix solution (2,5-dihydroxybenzoic acid, 10 mg ml^{-1} in aqueous 50% (v/v) acetonitrile, 1 µl) on the stainless steel MALDI target plate and concentrated to dryness using a flow of warm air from a hair dryer. Spectra from at least 200 laser shots were summed up to generate each mass spectrum.

2.9 Enzymatic hydrolysis

The enzymatic hydrolysis was reported previously and was used in a slightly modified form (vom Stein et al., 2011). Sida AIR, the extracted AIR and Avicel® (20 g L^{-1}), a model substrate for crystalline cellulose, were suspended in 0.1 M sodium citrate, pH 4.5 (10 ml, containing 0.01% sodium azide) at 50°C. Accellerase-1500® (1% (v/v)) exhibits strong cellulase and β-glucosidase activity to break down cellulose into fermentable glucose and was then added. Aliquots of the reactions (0.3 ml) and control (no enzyme added, 1 ml) were collected at 0 h, 1 h, 3 h, 6 h and 24 h. Enzymes were heat-inactivated (100°C). Glucose content was determined using the Glucose (HK) Assay Kit (Sigma-Aldrich).

The total glucan content represents the sum of glucose content determined for starch, MPS and crystalline cellulose (CrC). The glucose content of MPS and CrC was determined as previously described (Jablonowski et al., 2016) while glucose content of starch was determined by the Glucose (HK) Assay Kit (Sigma-Aldrich) after enzymatic hydrolysis with α-amylase (3 U) and amyloglucosidase (1.5 U) (Megazyme, Bray, Ireland).

3 Results and discussion

3.1 From glycosyl composition to polysaccharide structure

A greater understanding of plant cell wall architecture can contribute to the development of processes for the utilization of lignocellulose. In this study, we have used multiple analytical techniques to reveal the non-cellulosic polysaccharide composition and structure of Sida thereby providing insights into its cell wall architecture. A comparison of the saccharification efficiency of Sida in comparison to Avicel® provided an assessment of the recalcitrance of Sida biomass.

3.1.1 Biochemical characterization of Sida cell wall polysaccharides

Sida AIR was sequentially extracted with aqueous buffers and alkali to generate fractions enriched in hemicellulose and pectins. Ammonium oxalate was used first to solubilize cell

wall components including pectins. Carbonate, 1M KOH and 4M KOH were then used to solubilize more tightly bound cell wall glycans. The extracted AIR was then delignified using acidified sodium chlorite and finally treated with 4M KOH to solubilize cell wall polysaccharides that had been associated with lignin.

Table 1: Recovered material from *Sida hermaphrodita* AIR.

	mg material recovered/g AIR
Oxalate	18.9
Carbonate	12.1
1M KOH	243.1
4M KOH	196.3
Chlorite	40.8
4M KOHPC	285.1

The amounts of material recovered with each extraction are shown in Table 1. As expected for secondary cell walls and from previous studies (H. Li et al., 2014; M. Li, Pattathil, Hahn, & Hodge, 2014; Socha et al., 2014), the amount of recovered material was higher in alkaline extracts, with 4M KOHPC extract showing the highest followed by 1M KOH and 4M KOH. Approximately 3% of the AIR was solubilized by oxalate and carbonate. The overall amounts of pectic polysaccharides are much lower compared to the amount of hemicellulose or cellulose, which is typical for the secondary cell wall in most plants (Pauly et al., 2013; Scheller & Ulvskov, 2010).

The glycosyl residue and glycosyl-linkage compositions of each extract were then determined. The glycosyl compositions of each extract are shown in Table 2. Monosaccharides were assigned to different polysaccharides (Figure 1) based on the results of glycosyl-linkage analysis [supplementary material Table S1, (Pettolino, Walsh, Fincher, & Bacic, 2012)].

Table 2: Monosaccharide composition of the materials from sequentially extracted cell wall polysaccharides from Sida hermaphrodita AIR (n=2). Fractions were hydrolyzed with TFA and analyzed by HPAEC-PAD detection as described in the method section.

	Oxalate	Carbonate	1M KOH	4M KOH	Chlorite	4M KOHPC
Fucose (Fuc)	0.3 ± 0.0	0.1 ± 0.0	0.1 ± 0.0	1.2 ± 0.1	0.6 ± 0.0	0.6 ± 0.0
Rhamnose (Rha)	6.6 ± 0.2	2.2 ± 0.0	1.3 ± 0.0	1.9 ± 0.0	14.7 ± 0.0	4.2 ± 0.1
Arabinose (Ara)	11.6 ± 0.0	2.3 ± 0.1	0.4 ± 0.0	3.0 ± 0.0	20.1 ± 0.0	5.8 ± 0.1
Galactose (Gal)	8.8 ± 0.1	2.8 ± 0.0	0.8 ± 0.0	4.4 ± 0.0	22.4 ± 0.1	6.9 ± 0.0
Glucose (Glc)	34.7 ± 0.4	2.6 ± 0.1	5.2 ± 0.4	14.3 ± 1.5	8.6 ± 0.5	8.8 ± 0.1
Xylose (Xyl)	9.6 ± 0.3	83.3 ± 0.4	88.9 ± 0.7	65.9 ± 0.9	6.2 ± 0.2	62.5 ± 0.1
Mannose (Man)	4.7 ± 0.1	0.9 ± 0.0	0.5 ± 0.0	5.6 ± 0.4	0.5 ± 0.1	5.3 ± 0.0
Galacturonic Acid (GalA)	21.9 ± 0.6	5.2 ± 0.2	2.5 ± 0.3	3.5 ± 0.3	26.1 ± 0.0	5.6 ± 0.1
Glucuronic Acid (GlcA)	1.7 ± 0.1	0.6 ± 0.0	0.3 ± 0.0	0.2 ± 0.1	0.9 ± 0.0	0.3 ± 0.2

Numbers are the average (Mol%) ± SD.

The oxalate extract is dominated by glucose (Glc) and galacturonic acid (GalA) together with smaller amounts of arabinose (Ara), xylose (Xyl), galactose (Gal), rhamnose (Rha) and minor amounts of mannose (Man), glucuronic acid (GlcA) and fucose (Fuc). Almost half of the oxalate extract most likely consists of homogalacturonan (HG), rhamnogalacturonan I (RGI), arabinan and arabinogalactans (AG). Most of the glucan was likely derived from starch as the oxalate fraction contained only minor amounts of xyloglucan (XG). This is consistent with the results of glycosyl-linkage analysis and glycome profiling which is described in section 3.1.2. The arabinan is predominantly 5-linked and unbranched due to the lack of detectable 2,5-linked Ara *(*furanose (*f*)). The amounts of 2-Gal and terminal (t-) Fuc suggest the presence of decorated XG structures whereas t-Fuc could also derive from pectin.

The carbonate and 1M KOH extracts were dominated by Xyl (Table 2), which could nearly completely be assigned to xylan. In the carbonate extract, the reduced frequency of 2,4-linked Xyl residue (supplementary material Table S1) suggested that the number of branching points was lower than in the 1M KOH extract though the detected amounts of t-GlcA and t-Ara(*f*) did not reflect this tendency suggesting decoration apart from t-GlcA and t-Ara(*f*).

The 4M KOH extract also contained large amounts of Xyl. Substantial amounts of Glc together with 4-Man and 4,6-Man indicate that Sida stem walls additionally contain heteromannan (HM). The amount of HM in the 4M KOH extract was relatively high, which suggests that a portion of the HM is tightly bound to the cell wall. Residual amounts of 4-Glc are possibly part of XG and amorphous regions of cellulose, respectively. The 4M KOH extract also contained arabinan, AG, RG and HG.

Treatment with acidified chlorite oxidatively cleaves phenolic residue (lignin) in the cell wall and releases compounds, which were strongly associated with or bound to lignin (Pattathil, Avci, Zhang, Cardenas, & Hahn, 2015). Studies on corn-, rice stover and Miscanthus suggest that hemicelluloses especially xylan are the dominant connection to lignin (De Souza et al., 2015; De Souza, Leite, Pattathil, Hahn, & Buckeridge, 2013). However, Ara, Gal and GalA were the predominant monosaccharides in the chlorite solubilized material with only small amounts of Xyl and Glc (Table 2). Based on the linkage analysis, these polysaccharides were possibly RGI, arabinan, HG and AG. 85% (6.2 ± 0.3 mg recovered residue/g AIR) less material was recovered when the base-extracted material was treated with hot acetic acid only indicating that the majority of the material present in the chlorite fraction (supplementary material Table S2) is associated with, covalently bound to or coated by lignin. This led us to the assumption that pectic polysaccharides are the most abundant lignin-associated glycans compared to other non-cellulosic glycans. There is evidence for crosslinks between phenolic molecules and polysaccharides though primary cell walls were analyzed; Gal and Ara containing side chains can be feruloylated and might mediate this links (Fry, 1982, 1983) but also connection to other components have been described (Cathala, Chabbert, Joly, Dole, & Monties, 2001). However, if this can be transferred to Sida as well is not sure. Only a small part appeared to be xylan and XG (Figure 1). The higher amounts of 2,4-linked Rha suggest that the RGI solubilized by chlorite is more branched than the RGI in the other extracts.

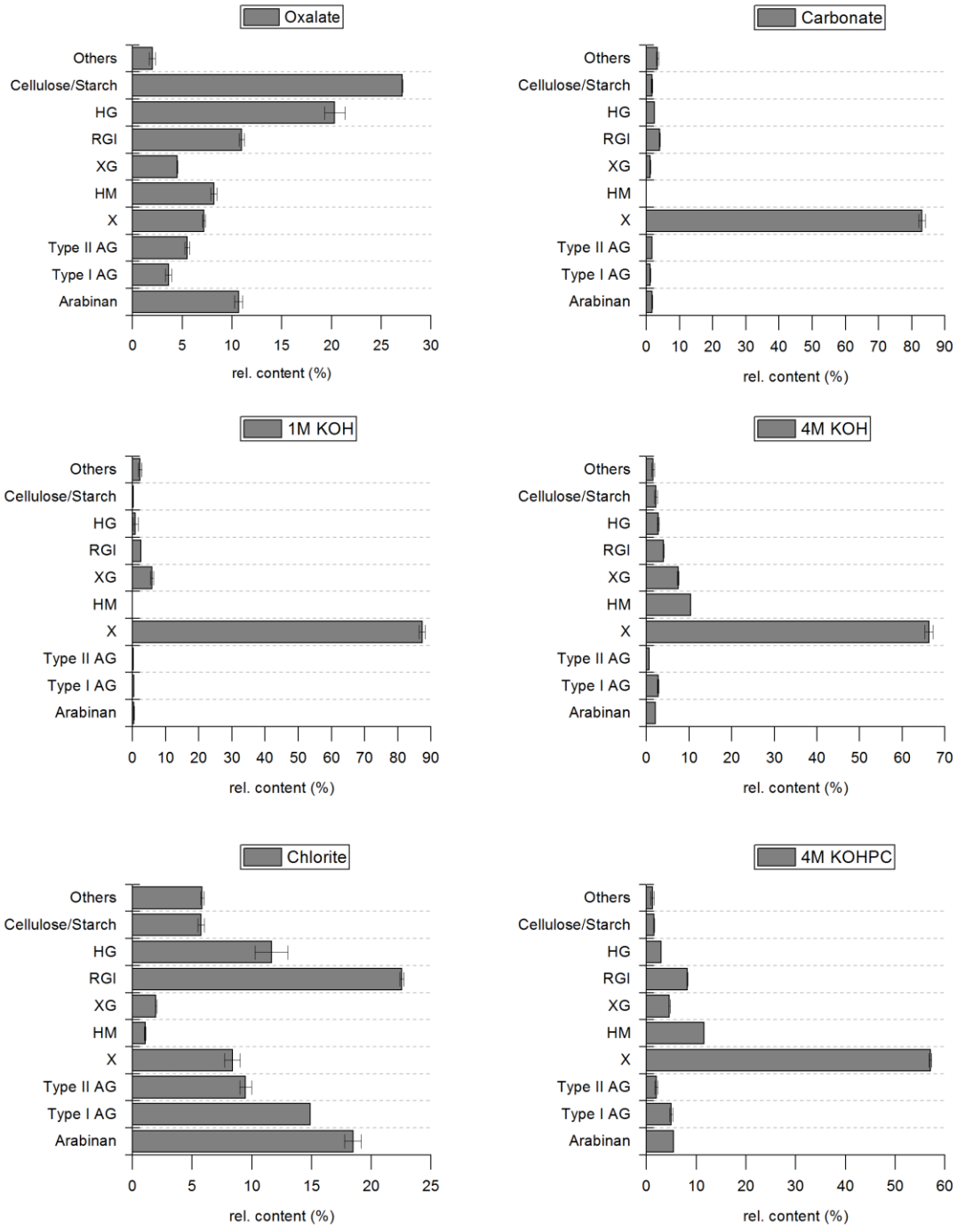

Figure 1: Polysaccharide compositions of *Sida hermaphrodita* assigned from glycosyl-linkage analyses of sequentially extracted cell wall polysaccharides as described in method section (n=2). Bars represent the aundance within each extract (%) ± SD. AG, arabinogalactan; HX, homoxylan; HM, heteromannan; XG, xyloglucan; RGI; rhamnogalacturonan I; HG, homogalacturonan.

The material solubilized by 4M KOH treatment of the chlorite-treated AIR was mostly composed of Xyl whereas the remaining monosaccharides are distributed equally (Table 2). Linkage analysis identified xylan as main component with a comparable degree of backbone

substitution as in the 4M KOH extract. To some extent, HM was again detected whereas other polysaccharides showed lower abundance (Figure 1).

The biochemical characterization identified xylan as the predominant non-cellulosic polysaccharide in the Sida stem cell wall. It has a relatively low number of branching points (ratio 4-Xyl to 2,4-Xyl of 20 to 1) with the highest branching pattern in the 1M KOH extract. A substantial part of the association from polysaccharide to lignin may be mediated through pectic polysaccharides rather than hemicelluloses. XG was detected only in small amounts in the biochemical analysis, which is consistent with the low abundance of XG in mature tissues that contain a high proportion of secondary cell walls (Vogel, 2008).

3.1.2 Glycome profiling of sequentially extracted cell wall polysaccharides

Glycome profiling (Figure 2) was performed on the extracts of Sida stem AIR to obtain an understanding of the types of cell wall polysaccharide that comprise the major non-cellulosic glycans.

XG epitopes were detected in all KOH extracts with the 4M KOH and 4M KOHPC extracts showing similar and broad pattern of XG epitope abundances. The 4M KOH and 4M KOHPC extracts contained XG epitopes that lack fucose recognized by all non-fucosylated XG groups of mAbs (non-fucosylated XG-1 through 6) with the exception of CCRC-M49 (from non-fucosylated XG-5 clade) that did not show binding. XG epitopes recognized by the Xylan-1/XG groups of mAbs were abundant in the extracts with the exception of the epitopes recognized by CCRC-M111. Epitopes that recognize regions of XG that lack fucose (XG-1 through 4), were detected in the 1M KOH extracts. The 1M KOH, 4M KOH and 4M KOHPC extracts all contained fucosylated XG epitopes. Biochemical data exhibited low amounts of t-Fuc but no 2-Xyl. Therefore additional analysis for verification was used and will be subsequently shown and discussed.

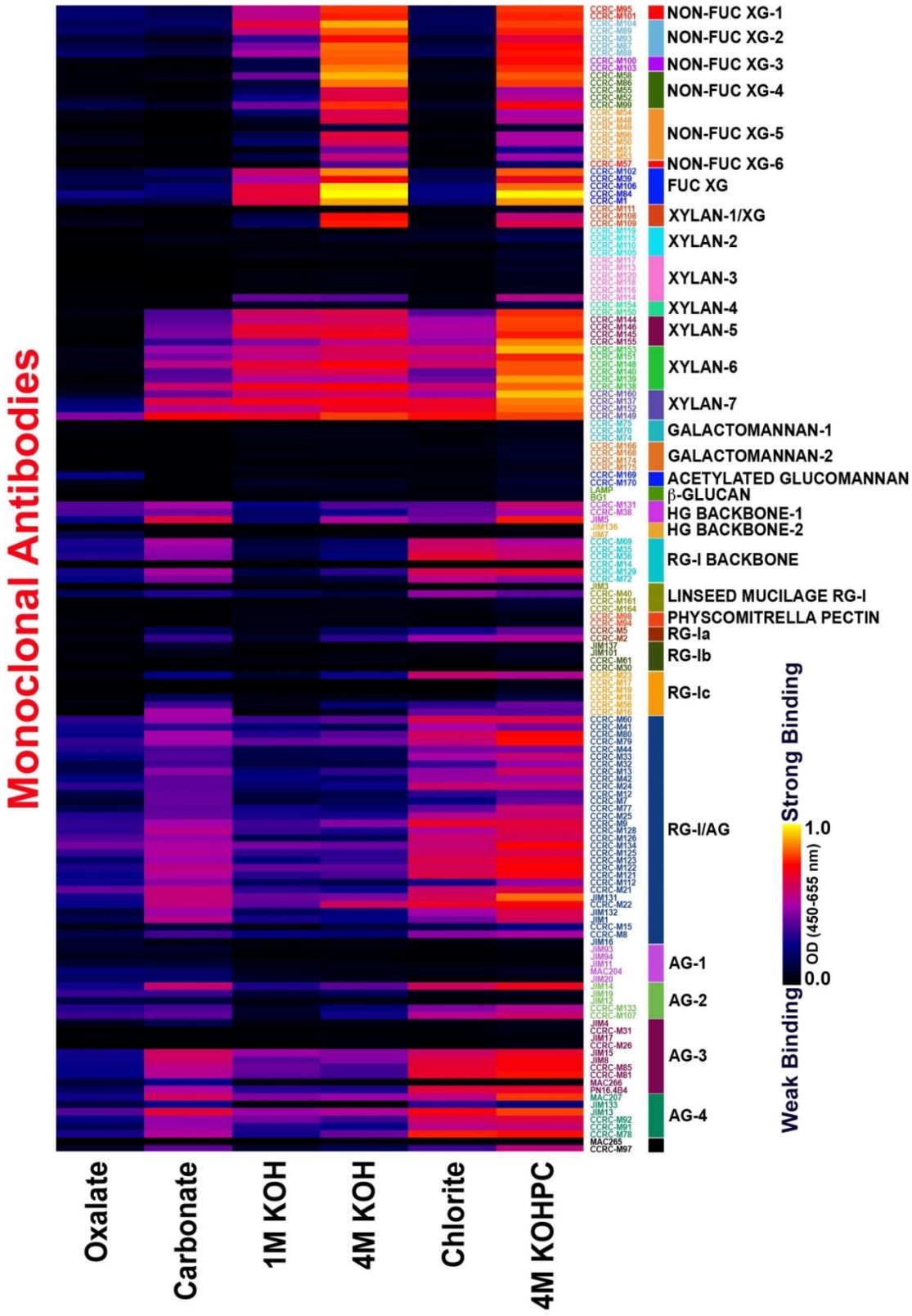

353

354 **Figure 2:** Glycome profiling of *Sida hermaphrodita* cell walls. Cell walls were isolated as the AIR, from *Sida*
355 *hermaphrodita* stems. Sequential extracts were probed for the presence using glycan-directed mAbs (Pattathil,
356 Avci, Miller, & Hahn, 2012). The intensity of the response of each mAbs are represented as a heat map with the
357 highest response in bright yellow to intermediate response in red and no response in black. The glycans
358 recognized by mAb groups are depicted in the right hand side panel.

Epitopes of un-substituted xylan and substituted regions of xylans were detected in all extracts except the oxalate extract in which xylan epitopes recognized by three mAbs of xylan-7 groups (namely, CCRC-M137, CCRC-M152 and CCRC-M149) were detected. This is in accordance with the glycosyl-linkage analysis and is supported by the signals of anti-xylan antibodies from group 6 and 7 which are specific for linear, unsubstituted epitopes (De Souza et al., 2013; Schmidt, Schuhmacher, Geissner, Seeberger, & Pfrengle, 2015). Arabinosylated xylan epitopes recognized by CCRC-M154 were not detected in any of the extracts. Epitopes recognized by mAbs specific to methyl-GlcA substituted xylan epitopes (xylan-5 group mAbs) were detected in all extracts except oxalate extracts. The presence of xylan epitopes in the chlorite and 4M KOHPC extracts is consistent with the results of biochemical analysis and suggests that xylan may also interact with lignin in Sida cell walls.

HG and RGI backbone (notably those recognized by HGI and RGI backbone groups of mAbs), pectic-arabinogalactan (as recognized by RGI/AG groups of mAbs) and arabinogalactan (AGI through 4 groups of mAbs) epitopes displayed similar pattern of extractability with their presence in all extracts. However, their abundances among extracts varied, with substantially higher abundances of these epitopes observed in the carbonate, chlorite and 4M KOHPC extracts. The abundance of pectic-backbone and pectic-arabinogalactan epitopes in the chlorite and 4M KOHPC extracts suggests that pectic polysaccharides, together with glucuronoxylans, interact with lignin in the Sida cell wall which is in accordance with data from the biochemical characterization. Additional information about individual mAbs employed in glycome profiling and showing a high and a medium signal towards Sida epitopes is provided (supplementary material Table S3/S4).

To verify our data for the presence of fucosylated xyloglucan obtained by glycosyl-linkage analysis and glycome profiling, the 4M KOH and the 4M KOHPC extract were treated with a xyloglucan-specific endoglucanse (XEG) and the products generated analyzed by MALDI-TOF-MS.

The MALDI-TOF-MS of the XEG-treated materials contained ions consistent with the presence of non-fucosylated and fucosylated XG subunits (Figure 3). Assigned structures are XXFG and XLFG of which XLFG had the higher abundance. These are typical structures which are present in Arabidopsis and many other dicot XGs (Pauly et al., 2013). Additional subunits were XXXG with the highest abundance and XXLG/XLXG with the lowest. These subunits are consistent with fucosylated xyloglucans found in many dicots (Neumetzler et al., 2012).

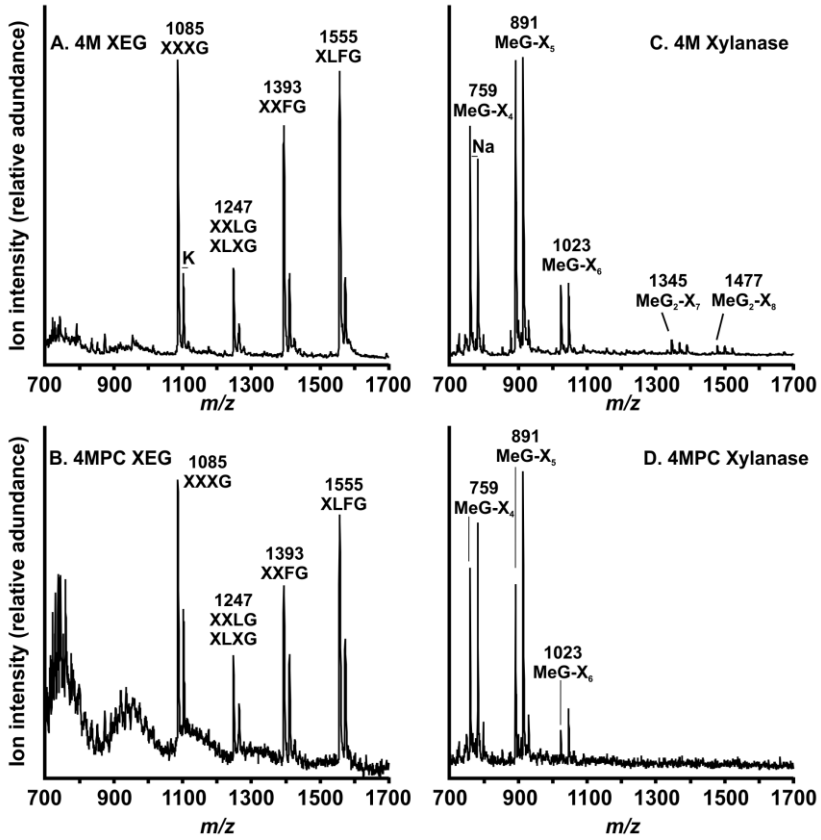

Figure 3: MALDI-TOF-MS of xyloglucan-specific endo-β-1,4-glucanase (XEG) - and xylanase-generated fragments of *Sida hermaphrodita* extracts were purified and analysed by MALDI-TOF-MS as described in the method section. Graphs represent the relative abundance of ion intensity for different fragment sizes. A/C, 4M KOH extract; B/D, 4M KOHPC extract; A/B, treated with XEG; C/D, treated with xylanase. Xyloglucans are classified as several types with a β-1,4-d-Glc backbone whose Glc (G) are unbranched or substituted with Xyl (X, Xyl 1,6-Glc). Xyl can further be substituted by Gal or Gal and Fuc (L, Gal 1,2-Xyl 1,6-Glc; F, Fuc 1,2-Gal 1,2-Xyl 1,6-Glc). Glucuronoxylan is classified as a β-(1→4)-linked xylose backbone substituted by α-(1→2)-linked glucuronosyl and 4-*O*-methyl glucuronosyl residue.

The most abundant polysaccharide in all 4M and 4MPC KOH extracts was xylan. To refine the previous analyses and gain additional evidence about branching and the degree of substitution, the two extracts were treated with an endoxylanase and the fragments were

analyzed by MALDI-TOF-MS. Xylanase treated samples showed typical 4-*O*-methyl glucuronoxylan where most of the GlcA is 4-O-methylated. The relative abundance of ions for MeGlcA-Xyl4 and MeGlcA-Xyl5 suggests that most of the MeGlcA is terminal – little if any Ara-MeGlcA side chain is likely to be present.

3.2 Non-cellulosic cell wall structure effecting enzymatic hydrolysis

As efficient pretreatment and fractionation of lignocellulose is limited by cell wall recalcitrance defined as the resistance of the plant material to deconstruction into fermentable sugars (Damm et al., 2016; Himmel & Picataggio, 2008; McCann & Carpita, 2015) we were interested in how non-cellulosic cell wall structures are effecting enzymatic hydrolysis of Sida cell walls.

We used Accellerase®-1500 to compare enzymatic hydrolysis of Sida AIR, extracted Sida AIR and Avicel® (Figure 4).

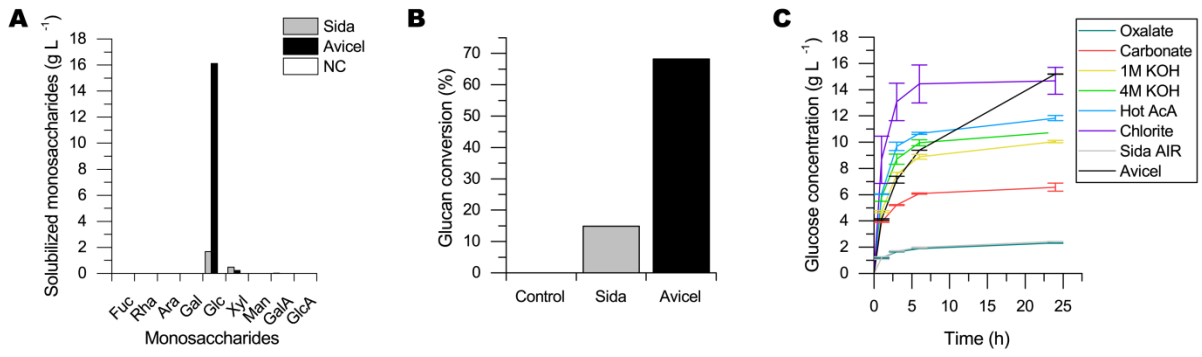

Figure 4: Enzymatic hydrolysis for *Sida hermaphrodita* stem AIR (n=5) and extracted AIR (n=2) in comparison to Avicel® (n=2). The enzymatic hydrolysis was conducted and evaluated using Accellerase®-1500. A, Amounts of monosaccharides solubilized after treatment with Accellerase®-1500 (mean t24-t0); B, Glucan conversion after 24 h; C, Enzymatic hydrolysis of sequentially extracted residues as well as Sida AIR and Avicel® as controls (n=2) were performed and respective glucose concentrations are shown. Hot AcA: Hot acetic acid without sodium chlorite used for extraction.

Solubilized monosaccharides were determined by HPAEC-PAD (Figure 4, A). Beside Glc smaller amounts of Xyl were solubilized during enzymatic hydrolysis. Focusing on Sida the glucose to xylose ratio is 3.4 to 1. Based on the total measured glucan in the Sida AIR, the amount of glucan conversion was calculated (Figure 4; B). The glucan conversion for Sida comprises 21% of that observed for Avicel®. To assess the influence of non-cellulosic cell wall structures on enzymatic hydrolysis we extracted Sida AIR as described within the method section and hydrolyzed the remaining residue with Accellerase®-1500 (Figure 4, C).

After 24 h the oxalate-treated residue and the untreated Sida material exhibited similar Glc yields (~2 g L^{-1}). Solubilizing small amounts of predominantly pectic polysaccharides like HG, RGI and AGs, does not appear to affect glucose release. By contrast, treatment with dilute alkali (50mM $NaCO_3$) increased the digestibility about 3-fold (<6 g L^{-1}). This is comparable to other studies where pretreatment with 5% NaOH for Sida is sufficient to increase subsequent methane production over >70% (Michalska, Bizukojć, & Ledakowicz, 2015). Carbonate extraction as well as KOH extractions mainly solubilized xylan and increased Sida digestibility. Glycome profiling and biochemical analyses indicated that KOH extraction solubilized highly branched xylan whereas in the carbonate fraction the amount and the number of branches were considerably lower. Extracting smaller amounts of more linear xylan with carbonate already increased the digestibility. To achieve even higher Glc yields, the highly branched xylan has to be removed by KOH extraction. Highest Glc yields after 24 h (<16 g L^{-1}) were obtained from material treated with acidified sodium chlorite. Chlorite treatment oxidizes aromatic residue in lignin and may hydrolyze acid-labile Ara(*f*) side branches (DeMartini et al., 2013b). The positive effect of lignin removal on enzymatic digestibility is well established and has been intensively studied (McCann & Carpita, 2015). Chlorite treatment improved the enzymatic digestibility of poplar more than of switchgrass (DeMartini et al., 2013b). Sida treated with chlorite showed a similar improvement as observed for poplar. Chlorite treatment of Sida cell wall residue also released small amounts of pectin suggesting that these polysaccharides may be associated with lignin. Similar

454 results were observed with poplar and loblolly pine (DeMartini et al., 2013b; Pattathil et al.,
455 2016) thus in this respect, Sida is more comparable to hard woods and softwoods than to
456 switchgrass or Miscanthus (De Souza et al., 2015) not surprising since Sida and populus are
457 both eudicots. Grasses including switchgrass, Miscanthus and sugarcane exhibited highly
458 increased digestibility after alkaline pretreatment and xylan removal (De Souza et al., 2015,
459 2013; DeMartini et al., 2013b). KOH hydrolyzes ester bonds. Especially, the de-esterification
460 of the ferulic acid linkage of glucuronoarabinoxylan to lignin in grasses can contribute to
461 higher digestibility (Buanafina et al., 2015). In dicotyledonous plants like Sida and Poplar, the
462 removal of xylans with KOH may be less effective due to the lack of phenolic ester linkages
463 between lignin and carbohydrates. This study strongly suggests that different strategies will
464 likely be necessary to pretreat Sida biomass than common bioenergy crops like switchgrass
465 or Miscanthus.

466 # 4 Conclusion

467 The data presented here provide a valuable resource for breeding strategies to increase the
468 potential of Sida as an energy crop. Furthermore, our study outlines the necessity for
469 different or modified processing strategies to efficiently convert Sida biomass. The provided
470 data can be used to develop tailored pretreatment and fractionation procedures to remove
471 specific cell wall components that restrict enzymatic digestibility, as well as to develop
472 improved enzymes to overcome the recalcitrant structures remaining after biomass
473 pretreatment. Both are important to increase the sustainability and economic feasibility of
474 lignocellulosic biomass utilization.

475 # 5 Acknowledgements

476 This work was realized within the project OrCaCel, kindly funded by the Bioeconomy
477 Science Center (BioSC). The scientific activities of the Bioeconomy Science Center were
478 financially supported by the Ministry of Innovation, Science and Research within the

framework of the NRW Strategieprojekt BioSC (No. 613 313/323-400-002 13). Glycome profiling experiments were supported by BioEnergy Science Center (BESC) administered by Oak Ridge National Laboratory and funded by a grant (DE-AC05-00OR22725) from the Office of Biological and Environmental Research, Office of Science, United States, Department of Energy. Enzymatic characterization of xyloglucan and xylan was funded through the Office of Basic Energy Sciences of the U.S. Department of Energy through Grant DE-FG02-12ER16324. The generation of the CCRC series of plant cell wall glycan-directed monoclonal antibodies used in this work was supported by the NSF Plant Genome Program (DBI-0421683 and IOS-0923992). We thank Genencor (The Netherlands) for kindly donating Accellerase-1500®.

6 References

Borkowska, H., & Molas, R. (2012). Two extremely different crops, Salix and Sida, as sources of renewable bioenergy. *Biomass and Bioenergy*, *36*, 234–240.

Borkowska, H., & Molas, R. (2013). Yield comparison of four lignocellulosic perennial energy crop species. *Biomass and Bioenergy*, *51*, 145–153.

Borkowska, H., Molas, R., & Kupczyk, A. (2009). Virginia Fanpetals (*Sida hermaphrodita* Rusby) Cultivated on Light Soil; Height of Yield and Biomass Productivity. *Polish Journal of Environmental Studies*, *18*(4), 563–568.

Buanafina, M. M. de O., Dalton, S., Langdon, T., Timms-Taravella, E., Shearer, E. A., & Morris, P. (2015). Functional co-expression of a fungal ferulic acid esterase and a β-1,4 endoxylanase in *Festuca arundinacea* (tall fescue) modifies post-harvest cell wall deconstruction. *Planta*, *242*(1), 97–111.

Cathala, B., Chabbert, B., Joly, C., Dole, P., & Monties, B. (2001). Synthesis, characterisation and water sorption properties of pectin-dehydrogenation polymer (lignin model compound) complex. *Phytochemistry*, *56*, 195–202.

Damm, T., Commandeur, U., Fischer, R., Usadel, B., & Klose, H. (2016). Improving the utilization of lignocellulosic biomass by polysaccharide modification. *Process Biochemistry*, *51*(2), 288–296.

De Souza, A. P., Kamei, C. L. A., Torres, A. F., Pattathil, S., Hahn, M. G., Trindade, L. M., & Buckeridge, M. S. (2015). How cell wall complexity influences saccharification efficiency in *Miscanthus sinensis*. *Journal of Experimental Botany*, *66*(14), 4351–4365.

De Souza, A. P., Leite, D. C. C., Pattathil, S., Hahn, M. G., & Buckeridge, M. S. (2013). Composition and Structure of Sugarcane Cell Wall Polysaccharides: Implications for Second-Generation Bioethanol Production. *Bioenergy Research*, *6*(2), 564–579.

DeMartini, J. D., Pattathil, S., Miller, J. S., Li, H., Hahn, M. G., & Wyman, C. E. (2013a). Investigating plant cell wall components that affect biomass recalcitrance in poplar and switchgrass. *Energy & Environmental Science*, *6*(3), 898.

DeMartini, J. D., Pattathil, S., Miller, J. S., Li, H., Hahn, M. G., & Wyman, C. E. (2013b). Investigating plant cell wall components that affect biomass recalcitrance in poplar and switchgrass. *Energy & Environmental Science*, *6*(3), 898.

Fornalé, S., Capellades, M., Encina, A., Wang, K., Irar, S., Lapierre, C., … Caparrós-Ruiz, D. (2012). Altered Lignin Biosynthesis Improves Cellulosic Bioethanol Production in Transgenic Maize Plants Down-Regulated for Cinnamyl Alcohol Dehydrogenase. *Molecular Plant*, *5*(4), 817–830.

Foster, C. E., Martin, T. M., & Pauly, M. (2010a). Comprehensive Compositional Analysis of Plant Cell Walls (Lignocellulosic biomass) Part I: Lignin. *Journal of Visualized Experiments : JoVE*, (37), 5–8.

Foster, C. E., Martin, T. M., & Pauly, M. (2010b). Comprehensive Compositional Analysis of Plant Cell Walls (Lignocellulosic biomass) Part II: Carbohydrates. *Journal of Visualized Experiments : JoVE*, (37), 2–5.

529 Franzaring, J., Holz, I., Kauf, Z., & Fangmeier, A. (2015). Responses of the novel bioenergy
530 plant species Sida hermaphrodita (L.) Rusby and Silphium perfoliatum L. to CO2
531 fertilization at different temperatures and water supply. *Biomass and Bioenergy*, *81*,
532 574–583.

533 Fry, S. C. (1982). Phenolic components of the primary cell wall: Feruloylated disaccharides
534 of D-galactose and L-arabinose from spinach polysaccharide. *Biochemical Journal*,
535 *203*(2), 493–504.

536 Fry, S. C. (1983). Feruloylated pectins from the primary cell wall: their structure and possible
537 functions. *Planta*, *157*(2), 111–123.

538 Gibeaut, D. M., & Carpita, N. C. (1991). Tracing Cell Wall Biogenesis in Intact Cells and
539 Plants: Selective Turnover and Alteration of Soluble and Cell Wall Polysaccharides in
540 Grasses. *Plant Physiology*, *97*(2), 551–61.

541 Gille, S., Hänsel, U., Ziemann, M., & Pauly, M. (2009). Identification of plant cell wall mutants
542 by means of a forward chemical genetic approach using hydrolases. *Proceedings of the*
543 *National Academy of Sciences of the United States of America*, *106*(34), 14699–14704.

544 Himmel, M. E., Ding, S.-Y., Johnson, D. K., Adney, W. S., Nimlos, M. R., Brady, J. W., &
545 Foust, T. D. (2007). Biomass Recalcitrance: Engineering Plants and Enzymes for
546 Biofuels Production. *Science*, *315*(5813), 804–807.

547 Himmel, M. E., & Picataggio, S. K. (2008). Our Challenge is to Acquire Deeper
548 Understanding of Biomass Recalcitrance and Conversion. In *Biomass Recalcitrance*
549 (pp. 1–6). inbook, Oxford, UK: Blackwell Publishing Ltd.

550 Huang, J., DeBowles, D., Esfandiari, E., Dean, G., Carpita, N. C., & Haughn, G. W. (2011).
551 The Arabidopsis Transcription Factor LUH/MUM1 is Required for Extrusion of Seed
552 Coat Mucilage. *Plant Physiology*, *156*(2), 491–502.

553 Jablonowski, N. D., Kollmann, T., Nabel, M., Damm, T., Klose, H., Müller, M., … Schurr, U.
554 (2016). Valorization of Sida (*Sida hermaphrodita*) biomass for multiple energy
555 purposes. *GCB Bioenergy*.

556 Kocoń, A., & Matyka, M. (2012). Phytoextractive potential of *Miscanthus giganteus* and *Sida*
557 *hermaphrodita* growing under moderate pollution of soil with Zn and Pb. *Journal of*
558 *Food, Agriculture and Environment*, *10*(2), 1253–1256.

559 Li, F., Ren, S., Zhang, W., Xu, Z., Xie, G., Chen, Y., … Peng, L. (2013). Arabinose
560 substitution degree in xylan positively affects lignocellulose enzymatic digestibility after
561 various NaOH/H2SO4 pretreatments in Miscanthus. *Bioresource Technology*, *130*,
562 629–637.

563 Li, H., Pattathil, S., Foston, M. B., Ding, S.-Y., Kumar, R., Gao, X., … Wyman, C. E. (2014).
564 Agave proves to be a low recalcitrant lignocellulosic feedstock for biofuels production
565 on semi-arid lands. *Biotechnology for Biofuels*, *7*(1), 50.

566 Li, M., Pattathil, S., Hahn, M. G., & Hodge, D. B. (2014). Identification of features associated
567 with plant cell wall recalcitrance to pretreatment by alkaline hydrogen peroxide in
568 diverse bioenergy feedstocks using glycome profiling. *RSC Advances*, *4*(33), 17282–
569 17292.

570 Mast, B., Lemmer, A., Oechsner, H., Reinhardt-Hanisch, A., Claupein, W., & Graeff-
571 Hönninger, S. (2014). Methane yield potential of novel perennial biogas crops
572 influenced by harvest date. *Industrial Crops and Products*, *58*(April 2016), 194–203.

573 McCann, M. C., & Carpita, N. C. (2015). Biomass recalcitrance: a multi-scale, multi-factor,
574 and conversion-specific property. *Journal of Experimental Botany*, *66*(14), 4109–4118.

575 Michalska, K., Bizukojć, M., & Ledakowicz, S. (2015). Pretreatment of energy crops with
576 sodium hydroxide and cellulolytic enzymes to increase biogas production. *Biomass and*
577 *Bioenergy*, *80*, 213–221.

578 Neumetzler, L., Humphrey, T., Lumba, S., Snyder, S., Yeats, T. H., Usadel, B., … Bonetta,
579 D. (2012). The FRIABLE1 Gene Product Affects Cell Adhesion in Arabidopsis. *PLoS*
580 *ONE*, *7*(8).

581 Packer, N. H., Lawson, M. A., Jardine, D. R., & Redmond, J. W. (1998). A general approach
582 to desalting oligosaccharides released from glycoproteins. *Glycoconjugate Journal*,
583 *15*(8), 737–747.

584 Pattathil, S., Avci, U., Miller, J. S., & Hahn, M. G. (2012). Immunological Approaches to Plant
585 Cell Wall and Biomass Characterization: Glycome Profiling. In E. M. Himmel (Ed.),
586 *Biomass Conversion: Methods and Protocols* (pp. 61–72).

587 Pattathil, S., Avci, U., Zhang, T., Cardenas, C. L., & Hahn, M. G. (2015). Immunological
588 Approaches to Biomass Characterization and Utilization. *Frontiers in Bioengineering*
589 *and Biotechnology*, *3*.

590 Pattathil, S., Ingwers, M. W., Victoriano, O. L., Kandemkavil, S., McGuire, M. A., Teskey, R.
591 O., & Aubrey, D. P. (2016). Cell Wall Ultrastructure of Stem Wood, Roots, and Needles
592 of a Conifer Varies in Response to Moisture Availability. *Frontiers in Plant Science*,
593 *7*(June), 882.

594 Pauly, M., Andersen, L. N., Kauppinen, S., Kofod, L. V, York, W. S., & Albersheim, P.
595 (1999). A xyloglucan-specific endo-β-1,4-glucanase from *Aspergillus aculeatus*:
596 expression cloning in yeast, purification and characterization of the recombinant
597 enzyme. *Glycobiology*, *9*(1), 93–100.

598 Pauly, M., Gille, S., Liu, L., Mansoori, N., de Souza, A., Schultink, A., & Xiong, G. (2013).
599 Hemicellulose biosynthesis. *Planta*, *238*(4), 627–642.

600 Pettolino, F. A., Walsh, C., Fincher, G. B., & Bacic, A. (2012). Determining the
601 polysaccharide composition of plant cell walls. *Nature Protocols*, *7*(9), 1590–1607.

602 Scheller, H. V., & Ulvskov, P. (2010). Hemicelluloses. *Annual Review of Plant Biology*, *61*,
603 263–89.

604 Schmidt, D., Schuhmacher, F., Geissner, A., Seeberger, P. H., & Pfrengle, F. (2015).
605 Automated Synthesis of Arabinoxylan-Oligosaccharides Enables Characterization of
606 Antibodies that Recognize Plant Cell Wall Glycans. *Chemistry - A European Journal*,
607 *21*(15), 5709–5713.

608 Scott, T. a., & Melvin, E. H. (1953). Determination of Dextran with Anthrone. *Analytical*
609 *Chemistry*, *25*(11), 1656–1661.

610 Šiaudinis, G., Jasinskas, A., Šarauskis, E., Steponavičius, D., Karčauskiene, D., &
611 Liaudanskiene, I. (2015). The assessment of Virginia mallow (*Sida hermaphrodita*
612 Rusby) and cup plant (Silphium perfoliatum L.) productivity, physico-mechanical
613 properties and energy expenses. *Energy*, *93*, 606–612.

614 Silveira, R. L., Stoyanov, S. R., Gusarov, S., Skaf, M. S., & Kovalenko, A. (2013). Plant
615 Biomass Recalcitrance : Effect of Hemicellulose Composition on Nanoscale Forces that
616 Control Cell Wall Strength. *Journal of the American Chemical Society*, (135),
617 19048−19051.

618 Slepetys, J., Kadziuliene, Z., Sarunaite, L., Tilvikiene, V., & Kryzeviciene, A. (2012). Biomass
619 potential of plants grown for bioenergy production. *International Scientific Conference:*
620 *Renewable Energy and Energy Efficiency*, 66–72.

621 Socha, A. M., Parthasarathi, R., Shi, J., Pattathil, S., Whyte, D., Bergeron, M., … Singh, S.
622 (2014). Efficient biomass pretreatment using ionic liquids derived from lignin and
623 hemicellulose. *Proceedings of the National Academy of Sciences of the United States*
624 *of America*, *111*(35), E3587–E3595.

625 Tollenaar, M., & Lee, E. A. (2002). Yield potential, yield stability and stress tolerance in
626 maize. *Field Crops Research*, *75*(2–3), 161–169.

627 Updegraff, D. M. (1969). Semimicro Determination of Cellulose in Biological Materials.
628 *Analytical Biochemistry*, *32*(3), 420–424.

629 Vogel, J. (2008). Unique aspects of the grass cell wall. *Current Opinion in Plant Biology*,
630 *11*(3), 301–307.

631 Voiniciuc, C., Schmidt, M. H.-W., Berger, A., Yang, B., Ebert, B., Scheller, H. V., … Günl, M.
632 (2015). MUCILAGE-RELATED10 Produces Galactoglucomannan That Maintains
633 Pectin and Cellulose Architecture in Arabidopsis Seed Mucilage. *Plant Physiology*,
634 *169*(1), 403–420.

635 vom Stein, T., Grande, P. M., Kayser, H., Sibilla, F., Leitner, W., & Domínguez de María, P.
636 (2011). From biomass to feedstock: one-step fractionation of lignocellulose components
637 by the selective organic acid-catalyzed depolymerization of hemicellulose in a biphasic
638 system. *Green Chemistry*, *13*(7), 1772.

639 Xiong, G., Cheng, K., & Pauly, M. (2013). Xylan O-Acetylation Impacts Xylem Development
640 and Enzymatic Recalcitrance as Indicated by the Arabidopsis Mutant tbl29. *Molecular*
641 *Plant*, *6*(4), 1373–1375.

642

643